

Turbulence in a Cylindrical Container of Argon near Threshold of Convection

A. Pocheau, V. Croquette, and P. Le Gal

*Service de Physique du Solide et de Résonance Magnétique, Centre d'Etudes Nucléaires de Saclay,
F-91191 Gif-sur-Yvette Cedex, France*

(Received 10 May 1985)

We present measurements and pattern visualization of convection in a cylindrical container at low Prandtl number. We demonstrate that the weak turbulence previously detected in this situation is clearly an erratic wandering of rolls. We show that the transition from a stationary to a time-dependent pattern involves spontaneous nucleation of dislocations. We analyze this phenomenon in relation to the skewed varicose instability.

PACS numbers: 47.25.Qv, 47.20.+m

The transition to time dependence in Rayleigh-Bénard convective patterns which are not spatially forced is still far from understood. In low-Prandtl-number N_{Pr} fluids ($N_{Pr} = \nu/\kappa$, where ν is the kinetic viscosity, and κ is the thermal diffusivity), experiments performed at cryogenic temperatures¹ on liquid helium ($0.5 < N_{Pr} < 0.8$) reveal time dependence at a Rayleigh number N_{Ra} slightly above the convection threshold N_{Ra}^c (specifically, $N_{Ra} \approx 1.1 * N_{Ra}^c$), where a stationary roll pattern is expected² ($N_{Ra} = \alpha g \delta T d^3 / \nu \kappa$, where α is the thermal expansion coefficient, g is the gravitational acceleration, and δT is the temperature difference applied to the fluid layer of depth d). Unfortunately in these experiments, contrary to those performed at room temperature, the associated patterns could not be visualized. Although surprising, these results were confirmed by further cryogenic experiments,³ and investigations in mercury⁴ at $N_{Pr} = 0.025$ demonstrated that these time-dependent states were related to pattern instabilities favored by small Prandtl number and cylindrical containers.

On the other hand, in convection experiments performed at room temperature with fluids of high Prandtl number (see Bergé⁵) turbulence is thought to occur only at much higher N_{Ra} —on the order of several times N_{Ra}^c —and appears as a complicated pattern after the growth of a secondary instability. At lower N_{Ra} , the pattern, now composed of rolls, often displays a long transient evolution involving defect motions before reaching a stationary and imperfect structure.⁶ This transient evolution suggests that a lowering of N_{Pr} might result in sustained erratic wandering of roll patches, called phase turbulence.⁵

Erratic wandering of rolls slightly above the convection threshold has recently been reported in water⁷ at $N_{Pr} = 2.5$ and 5. There, the time dependence observed in the pattern does not greatly affect the heat flux, and disappears when N_{Ra} is increased. Since at $N_{Pr} = 0.7$ ^{1,3} time dependence not only persists but accelerates with N_{Ra} , and is significantly reflected in the heat flux, the observations in water do not completely elucidate experimental results at lower Prandtl numbers.

We have performed experiments at room tempera-

ture using argon whose Prandtl number $N_{Pr} = 0.69$ is comparable to that of liquid helium. We have designed the apparatus so that we are able to measure the total heat flux transported by the convective layer. Moreover, working at a pressure of 30 bars, we have been able to visualize the convective pattern.

We have studied a cylindrical container with an aspect ratio $\Gamma = R/d$ equal to 7.66. In agreement with cryogenic experiments³ we found that, just above threshold, the convective pattern is stationary and we show that it is composed of straight rolls. At $\epsilon = 0.14$ [$\epsilon = (N_{Ra} - N_{Ra}^c) / N_{Ra}^c$], the pattern becomes time dependent through the occurrence of spontaneous nucleation of dislocations. This evolution is first periodic and rapidly becomes chaotic as we increase ϵ . The roll pattern then wanders erratically, exhibiting phase turbulence. We analyze the mechanism of this turbulence and observe that the roll diameters vary within a wide range bounded by the occurrence of dislocation nucleations for small rolls and by the appearance of small perpendicular rolls for large rolls. At higher ϵ , we observe the onset of oscillatory instability superimposed on the phase turbulence.

The visualization technique that we use relies on the usual shadowgraphic method,⁸ based on light-beam deviation induced by refractive-index gradients which result in turn from the temperature modulation in the convective layer. Since N_{Ra} grows like the square of the gas pressure (via ν and κ), the depth of the cell d may be reduced while keeping the critical temperature δT_c constant by increasing the pressure. This property is very advantageous since decreasing d magnifies the index gradients and facilitates the optical treatment of large-aspect-ratio containers. In particular, with a pressure of 30 bars we are able to use a depth of only 1.5 mm while retaining a critical temperature difference of 5.1 K.

The container consists of a Plexiglas ring 1 mm thick with an inner diameter of 23 mm, whose thermal conductivity is 9 times greater than that of argon. The vertical and horizontal diffusion times are short: $\tau_v = 3$ s and $\tau_h = 150$ s. The cell is sandwiched between a thermally regulated sapphire plate at the top and a copper mirror in contact with an electrical heater

at the bottom. This apparatus is placed in a pressurized vessel which is provided with a thick glass window for visualization. To avoid radiative losses, the copper mirror and its heater are surrounded by a thermal shield maintained at the same temperature. The power supplied by the heater then passes only through the convective layer and the container sidewall. In a preliminary experiment performed under vacuum, we have measured the sidewall contribution, in order to accurately determine the Nusselt number. We shall describe our apparatus in detail elsewhere.⁹

Near the threshold, up to $\epsilon=0.2$, the convective pattern appears to be uniquely determined by ϵ . At the threshold, it consists of straight and stationary rolls with identical widths [Fig. 1(a)]. The wave vector of the pattern is well defined and its value $k = 3.15 \pm 0.15$ is close to the critical value.

When ϵ is further increased, the rolls progressively bend, tending to become perpendicular to the sidewall. The structure, still stationary, then contains two focus

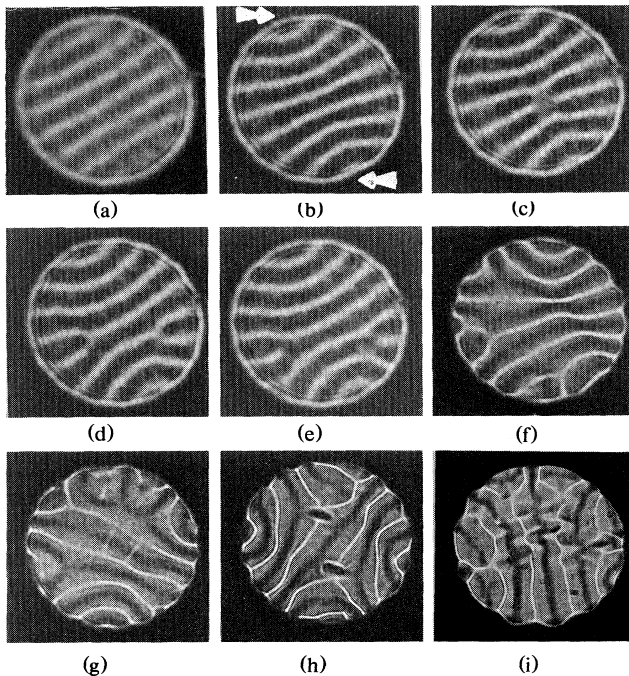


FIG. 1. Shadowgraphic pictures of convective patterns: (a) $\epsilon = 0.05$. Stationary straight-roll pattern. (b)–(c) $\epsilon = 0.14$. Description of one period of oscillation involving dislocation nucleations. The arrows in (b) indicate the center of focus singularities. (d)–(e) $\epsilon = 1$. Beginning of roll pinching occurring in a skewed manner on four adjacent wavelengths. (f) $\epsilon = 2$. Small perpendicular roll pairs growing on a large roll in the center of the cell. (g)–(h) $\epsilon = 3$. Simultaneous occurrence of small roll pairs near dislocations and roll pinchings. Notice the symmetry of this pattern. (i) $\epsilon = 4$. Oscillatory instability affecting relatively straight large rolls.

singularities as can be seen in Fig. 1(b). However, the roll diameters are no longer uniform so that only a local wave vector⁷ can be defined. We find its maximum value to be in the center of the cell and its minimum near the sidewall. The width of the wave-vector distribution of this stationary structure increases with ϵ (see Fig. 2), and at $\epsilon=0.14$ the local wave vector reaches the value of 3.6 in the center of the container. Then, as is shown in Fig. 1(c), two dislocations nucleate spontaneously there, as the result of a sudden pinching of the roll. They climb rapidly along the roll towards the sidewalls but eventually glide towards the focus singularities [Figs. 1(d) and 1(e)], where they disappear. The structure then relaxes to its initial state [Fig. 1(b)], as the focus singularities continuously generate new rolls. The same process may thus take place again, and indeed, no stationary structure could be found at higher ϵ . The way that the dislocations annihilate depends strongly on ϵ and rapidly becomes aperiodic. Each occurrence of dislocations, whether in a periodic or chaotic regime, produces a sharp peak in the heat flux, as shown in Fig. 3. This time-dependent behavior is, we believe, that observed in liquid helium.¹ The transition to chaos is very sensitive to the pattern features. For example, the characteristic period has the value $10\tau_h$ at $\epsilon=0.14$, but the value $35\tau_h$ at $\epsilon=0.18$ where the pattern consists of fourteen rather than fifteen rolls.

As we increase ϵ beyond 0.2, one dislocation

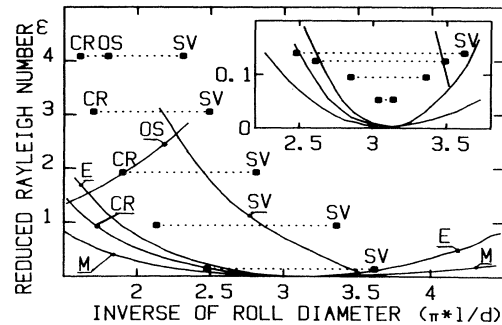


FIG. 2. Approximate roll-diameter distribution. The horizontal coordinate is given in units of $\pi l/d$ (l is the roll diameter) and coincides with the wave-vector definition for straight rolls. For a given ϵ , we have drawn a dotted line between the maximum and the minimum value determined from photographs. When an instability occurs, we have symbolized it by two letters (SV, skewed varicose; CR, cross roll; OS, oscillatory). As an indication we have reproduced the instability boundaries predicted for straight rolls (E, Eckhaus; M, marginal). This diagram is approximate since the roll diameters are measured on nonstationary patterns. However, we have also measured the evolution of the roll-diameter distribution vs ϵ on stationary and regular patterns as may be seen in the enlarged view of the threshold vicinity.

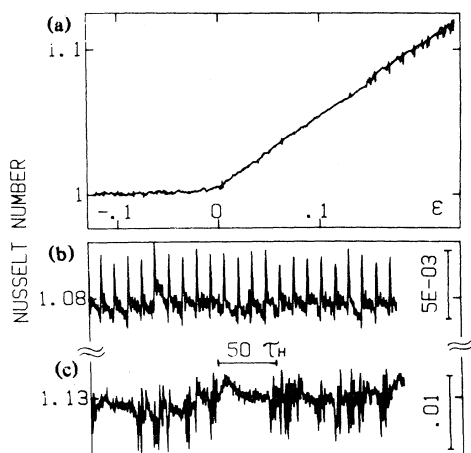


FIG. 3. Nusselt measurements: (a) Nusselt-number recording vs ϵ during a slow decreasing ramp in the threshold vicinity. Above $\epsilon = 0.14$ the recording is time dependent. (b), (c) Nusselt recordings vs time in (b) a periodic regime, $\epsilon = 0.14$, and (c) a chaotic regime, $\epsilon = 0.25$.

remains longer in the cell, often trapped at the sidewall, and sometimes succeeds in creating a third small focus singularity. As a result, the structure evolves chaotically through competition between patterns with two or three focus singularities. More generally, when ϵ is greater than 0.2, many topologically different structures appear successively at the same ϵ . The major events responsible for this time dependence are roll pinchings giving rise to spontaneous dislocation nucleations. These sudden events are separated by slow pattern relaxation.

A striking feature of these patterns is the large distribution of roll diameters, which increases with ϵ . Focus singularities "generate" rolls and thus tend to decrease their diameter until pinching occurs on the smallest rolls. However, starting at $\epsilon \approx 1$, pinching affects several wavelengths simultaneously. Moreover, it occurs obliquely with respect to the roll orientation [Fig. 1(f)], reminiscent of the skewed-varicose instability of Busse.² Meanwhile, for $\epsilon \approx 2$, a new mechanism of structural change also appears for the large-diameter rolls: Small roll pairs may grow perpendicular to them [Fig. 1(g)]. We interpret this as a localized cross-roll instability. This instability, which can cause grain boundary nucleation, frequently occurs at dislocations [Fig. 1(h)].

For ϵ greater than 2, the roll-diameter distribution may be so large that a structure may simultaneously display both the skewed-varicose- and cross-roll-like instabilities. Finally, beyond $\epsilon \approx 3.5$, the oscillatory straight rolls of large diameter, typically with a frequency of 1 Hz and a wave vector of $k_0 \approx 2.5$ as seen by Willis *et al.*¹⁰ As the pattern is already highly tur-

bulent this instability only adds some high frequencies to the dynamic.

In cylindrical containers with liquid helium, Behringer and Gao³ have inferred that the onset of time dependence coincides with the lowest (in ϵ) point of the skewed-varicose instability boundary. In water, Gollub *et al.*¹¹ have also shown how this instability leads to time-dependent patterns. At the onset of time dependence, we observe that under the strain of the focus singularities, the local wave vector in the center of the cell reaches roughly the skewed-varicose instability boundary (see Fig. 2). This route to turbulence is consistent with the predictions of Cross and Newell¹² and, in our experiment, involves periodic nucleation dislocations. Despite the fact that this mechanism cannot be regarded as the pure skewed-varicose instability defined for an infinite straight-roll pattern, Clever and Busse have already recognized it as the end result of the skewed-varicose instability.¹³ We explain how the wave vector attains the unexpectedly high value of 3.5 necessary to reach the skewed-varicose instability boundary, via a large distribution of roll diameters.

We found this distribution especially large compared to that observed at higher N_{Pr} .¹¹ This effect already appears for our stationary patterns and increases with ϵ so that the wave-number distribution finally fills the entire width of the Busse balloon. According to Clever and Busse¹³ the skewed-varicose instability should act as a wave-number-selection mechanism bringing the structure back inside the balloon, where the pattern should be stationary. Since, moreover, our patterns are turbulent inside this balloon, we doubt that a well-defined wave number is selected in our experimental situation.

To our knowledge there is no clear explanation of this turbulence, but only indirect approaches. Since the skewed-varicose instability is involved, large-scale flows are expected, as stressed by Cross.¹⁴ Indeed, Zippelius and Siggia have demonstrated theoretically that the stability of roll structures is drastically modified by these flows.¹⁵ This has been illustrated by Manneville in a numerical simulation¹⁶: The dislocation nucleations are preceded by a convergence of these flows. Moreover, the texturelike structure he observed at high N_{Pr} relaxes to a straight-roll pattern when N_{Pr} is decreased. This last point coincides well with the simplicity and the uniqueness of our stationary patterns observed up to $\epsilon = 0.14$. Manneville also suggests that this turbulence might be due to frustration between the large-scale flows and the convective structure linked to the cell geometry. Following these authors, we think that the large-scale flows might be related to the spread in the roll diameters giving rise to time dependence when a boundary of the Busse balloon is reached. We believe that this relation between

wave-vector distribution and large-scale flows has not yet been pointed out. Our hypothesis is supported by the similarity of their behavior in ϵ and N_{Pr} .

In light of the findings in rectangular containers¹⁷ where this kind of turbulence does not seem to occur, further study of the influence of the container symmetry, such as that in Ref. 4, would be fruitful.

In conclusion, we have shown that a nonperturbative visualization method is possible for low-Prandtl-number convective patterns. We have determined the mechanism responsible for turbulence occurring close to the convective threshold in a cylindrical container with $\Gamma = 7.66$. We emphasize the unusual roll-diameter distribution, and the role played by the skewed-varicose instability leading to spontaneous dislocation nucleations and thus to time dependence.

We have appreciated numerous discussions with P. Manneville, M. Dubois, P. Bergé, L. Tuckerman, Y. Pomeau, and the helpful advice of A. Schuhl, A. Pari, M. Hammann, G. Deneuille, C. Poitou, B. Ozenda, M. Labouise, B. Menetrier, and A. Guillot.

¹G. Ahlers and R. W. Walden, Phys. Rev. Lett. **44**, 445 (1980); R. P. Behringer and G. Ahlers, J. Fluid Mech. **125**, 219 (1982); A. Libchaber and J. Maurer, J. Phys. (Paris), Lett. **39**, L369 (1978).

²F. H. Busse, Rep. Prog. Phys. **41**, 1929 (1978); R. M. Clever and F. H. Busse, J. Fluid Mech. **65**, 625 (1974); F. H. Busse, J. Fluid Mech. **91**, 319 (1979).

³R. P. Behringer and H. Gao, Phys. Rev. Lett. **50**, 1199 (1983); H. Gao and R. P. Behringer, Phys. Rev. A **30**, 2837 (1984).

⁴S. Fauve, C. Laroche, A. Libchaber, and B. Perrin, Phys. Rev. Lett. **52**, 1774 (1984).

⁵P. Bergé, in *Chaos and Order in Nature*, edited by H. Haken, Springer Series in Synergetics, Vol. 11 (Springer-Verlag, New York, 1984).

⁶V. Croquette, M. Mory, and F. Schosseler, J. Phys. (Paris) **44**, 293 (1983).

⁷H. S. Heutmaker, P. N. Fraenkel, and J. P. Gollub, Phys. Rev. Lett. **54**, 1369 (1985); G. Ahlers, D. S. Cannell, and V. Steinberg, Phys. Rev. Lett. **54**, 1373 (1985).

⁸M. M. Chen and J. A. Whitehead, J. Fluid Mech. **31**, 1 (1968).

⁹A. Pocheau, V. Croquette, and P. Le Gal, to be published.

¹⁰G. E. Willis and J. W. Deardorff, J. Fluid Mech. **44**, 661 (1970); G. E. Willis, J. W. Deardorff, and R. C. Sommerville, J. Fluid Mech. **54**, 351 (1972).

¹¹V. Croquette and A. Pocheau, in *Cellular Structures in Instabilities*, edited by J. E. Wesfreid and S. Zaleski, Lecture Notes in Physics, Vol. 210 (Springer-Verlag, New York, 1984), p. 104; J. P. Gollub, J. F. Steinman, and A. R. McCarriar, J. Fluid Mech. **125**, 259 (1982); J. P. Gollub and A. R. McCarriar, Phys. Rev. A **26**, 2470 (1982).

¹²M. C. Cross and A. C. Newell, Physica (Amsterdam) **10D**, 299 (1984).

¹³R. M. Clever and F. H. Busse, Z. Angew. Math. Phys. **29**, 711 (1978).

¹⁴M. C. Cross, Phys. Rev. A **27**, 490 (1983).

¹⁵A. Zippelius and E. D. Siggia, Phys. Rev. A **26**, 1788 (1982), and Phys. Fluids **26**, 2905 (1983).

¹⁶P. Manneville, J. Phys. (Paris) **44**, 759 (1983), and J. Phys. (Paris), Lett. **44**, L903 (1983), and in *Cellular Structures in Instabilities*, edited by J. E. Wesfreid and S. Zaleski, Lecture Notes in Physics, Vol. 210 (Springer-Verlag, New York, 1984), p. 137.

¹⁷B. Martinet, P. Haldenwang, G. Labrosse, J. C. Payan, and R. Payan, J. Phys. (Paris), Lett. **43**, L161 (1982), and in *Cellular Structures in Instabilities*, edited by J. E. Wesfreid and S. Zaleski, Lecture Notes in Physics, Vol. 210 (Springer-Verlag, New York, 1984), p. 33.

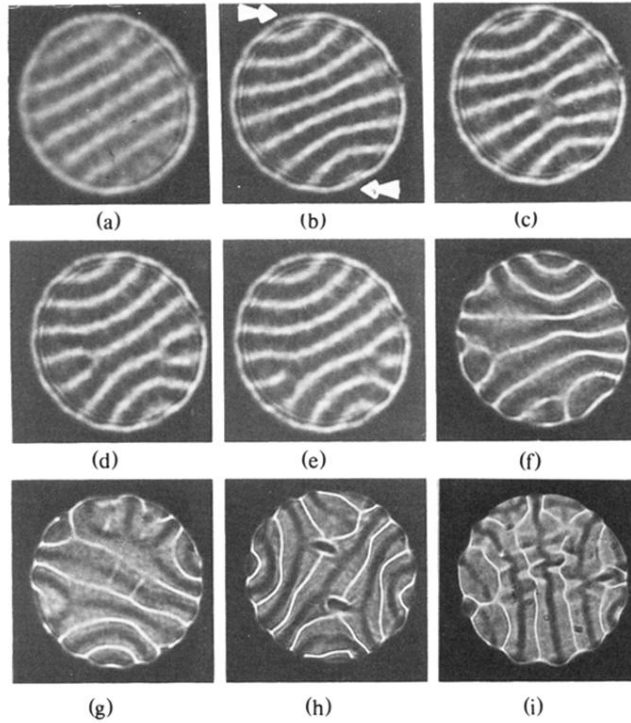


FIG. 1. Shadowgraphic pictures of convective patterns: (a) $\epsilon = 0.05$. Stationary straight-roll pattern. (b)–(e) $\epsilon = 0.14$. Description of one period of oscillation involving dislocation nucleations. The arrows in (b) indicate the center of focus singularities. (f) $\epsilon = 1$. Beginning of roll pinching occurring in a skewed manner on four adjacent wavelengths. (g) $\epsilon = 2$. Small perpendicular roll pairs growing on a large roll in the center of the cell. (h) $\epsilon = 3$. Simultaneous occurrence of small roll pairs near dislocations and roll pinchings. Notice the symmetry of this pattern. (i) $\epsilon = 4$. Oscillatory instability affecting relatively straight large rolls.